

RESEARCH ARTICLE

# The Phosphoinositide 3-Kinase p110 $\alpha$ Isoform Regulates Leukemia Inhibitory Factor Receptor Expression via c-Myc and miR-125b to Promote Cell Proliferation in Medulloblastoma

Fabiana Salm<sup>1</sup>\*, Valeriya Dimitrova<sup>1</sup>\*, André O. von Bueren<sup>2</sup>, Paulina Ćwiek<sup>1</sup>, Hubert Rehrauer<sup>3</sup>, Valentin Djonov<sup>4</sup>, Pascale Anderle<sup>5,6,7</sup>, Alexandre Arcaro<sup>1</sup>\*

**1** Department of Clinical Research, Division of Pediatric Hematology/Oncology, University of Bern, Bern, Switzerland, **2** Department of Pediatrics and Department of Pediatric Hematology and Oncology, Georg August University Goettingen, Goettingen, Germany, **3** Functional Genomics Center Zurich, ETH and University of Zurich, Zurich, Switzerland, **4** Institute of Anatomy, University of Bern, Bern, Switzerland, **5** Institute of Biochemistry and Molecular Medicine, University of Bern, Swiss National Centre of Competence in Research TransCure, University of Bern, Bern, Switzerland, **6** Swiss National Centre of Competence in Research Molecular Oncology, Swiss Institute for Experimental Cancer Research, Ecole Polytechnique Fédérale de Lausanne, School of Life Sciences, Lausanne, Switzerland, **7** Swiss Institute of Bioinformatics, Lausanne, Switzerland

\* These authors contributed equally to this work.

\* [alexandre.arcaro@dkf.unibe.ch](mailto:alexandre.arcaro@dkf.unibe.ch)



**OPEN ACCESS**

**Citation:** Salm F, Dimitrova V, von Bueren AO, Ćwiek P, Rehrauer H, Djonov V, et al. (2015) The Phosphoinositide 3-Kinase p110 $\alpha$  Isoform Regulates Leukemia Inhibitory Factor Receptor Expression via c-Myc and miR-125b to Promote Cell Proliferation in Medulloblastoma. PLoS ONE 10(4): e0123958. doi:10.1371/journal.pone.0123958

**Academic Editor:** Peter Hurlin, Shriners Hospitals for Children, UNITED STATES

**Received:** August 21, 2014

**Accepted:** February 26, 2015

**Published:** April 27, 2015

**Copyright:** © 2015 Salm et al. This is an open access article distributed under the terms of the [Creative Commons Attribution License](https://creativecommons.org/licenses/by/4.0/), which permits unrestricted use, distribution, and reproduction in any medium, provided the original author and source are credited.

**Data Availability Statement:** All relevant data are within the paper and its Supporting Information files.

**Funding:** This work was supported by a grant from the Fondation FORCE, Hartmann Müller-Stiftung, Ida de Pottère-Leupold-Fonds zur Förderung der Krebsforschung, Berner Stiftung für krebserkrankte Kinder und Jugendliche. The research leading to these results has received funding from the European Union's Seventh Framework Programme (FP7/2007–2013) under grant agreement No. 259348. The funders had no role in study design, data collection

## Abstract

Medulloblastoma (MB) is the most common malignant brain tumor in childhood and represents the main cause of cancer-related death in this age group. The phosphoinositide 3-kinase (PI3K) pathway has been shown to play an important role in the regulation of medulloblastoma cell survival and proliferation, but the molecular mechanisms and downstream effectors underlying PI3K signaling still remain elusive. The impact of RNA interference (RNAi)-mediated silencing of PI3K isoforms p110 $\alpha$  and p110 $\delta$  on global gene expression was investigated by DNA microarray analysis in medulloblastoma cell lines. A subset of genes with selectively altered expression upon p110 $\alpha$  silencing in comparison to silencing of the closely related p110 $\delta$  isoform was revealed. Among these genes, the leukemia inhibitory factor receptor  $\alpha$  (LIFR $\alpha$ ) was validated as a novel p110 $\alpha$  target in medulloblastoma. A network involving c-Myc and miR-125b was shown to be involved in the control of LIFR $\alpha$  expression downstream of p110 $\alpha$ . Targeting the LIFR $\alpha$  by RNAi, or by using neutralizing reagents impaired medulloblastoma cell proliferation *in vitro* and induced a tumor volume reduction *in vivo*. An analysis of primary tumors revealed that LIFR $\alpha$  and p110 $\alpha$  expression were elevated in the sonic hedgehog (SHH) subgroup of medulloblastoma, indicating its clinical relevance. Together, these data reveal a novel molecular signaling network, in which PI3K isoform p110 $\alpha$  controls the expression of LIFR $\alpha$  via c-Myc and miR-125b to promote MB cell proliferation.

and analysis, decision to publish, or preparation of the manuscript.

**Competing Interests:** The authors have declared that no competing interests exist.

## Introduction

Medulloblastoma is the most common malignant brain tumor in children and accounts for approximately 20% to 25% of all pediatric central nervous system tumors [1, 2]. Most medulloblastoma occur between 5 and 10 years of age [1, 3]. The standard treatment of medulloblastoma involves surgery followed by chemotherapy and, in the case of children older than 3–5 years, craniospinal radiotherapy [3]. However, nearly half of all patients die from progressive disease and the 5-year survival rate is below 50% for high-risk patients [2]. There is an urgent need to develop novel targeted therapeutic approaches for medulloblastoma, which will originate from a better understanding of the disease biology.

Medulloblastoma has been recognized to be a heterogeneous disease, and no recurrent cancer gene mutations have been found, although many of the mutations described so far affect key intracellular signaling pathways, such as sonic hedgehog (SHH) and Wnt/ $\beta$ -catenin [4, 5]. Genomic studies in large series of primary medulloblastoma have led to a novel classification of medulloblastoma into different molecular subtypes, characterized by the activation of sonic hedgehog (SHH), Wnt/ $\beta$ -catenin or c-Myc pathways (Group 3) [5]. c-Myc plays an important role in medulloblastoma biology and therefore targeting the signaling networks controlled by c-Myc may be a promising approach to develop targeted therapies for the subsets of tumors in which c-Myc is activated [6–11].

Another signaling pathway which is being considered to develop targeted therapies for medulloblastoma, is the receptor tyrosine kinase (RTK) cascade, which links polypeptide growth factors to cellular responses via their downstream signaling intermediates, in particular phosphoinositide 3-kinase (PI3K), Akt, the mammalian target of rapamycin (mTOR) and mitogen-activated extracellular signal-regulated kinase activating kinase (MEK) [12–18].

The PI3K signaling pathway controls key cellular responses, such as cell growth and proliferation, survival, migration and metabolism. Over the last decades, it has been recognized that this intracellular signaling pathway is frequently activated by genetic and epigenetic alterations in human cancer, including malignant brain tumors [4, 15, 19, 20]. The PI3K family of signaling enzymes comprises eight catalytic isoforms, which are subdivided into three classes. The class I<sub>A</sub> PI3K isoform p110 $\alpha$  is considered to be a validated drug target in human cancer, in particular because activating mutations in the *PIK3CA* frequently occur in human cancer [21, 22]. In medulloblastoma, the *PIK3CA* gene is targeted by mutations at a low frequency [23], but the p110 $\alpha$  isoform is also over-expressed in primary tumors and cell lines [15]. Our previous studies demonstrate the distinct roles of the class IA PI3K isoforms in medulloblastoma, from which p110 $\alpha$  showed the strongest effects in the control of medulloblastoma proliferation, survival and chemoresistance. Targeting p110 $\alpha$  by RNAi or isoform-specific inhibitors impaired medulloblastoma cell proliferation, survival and chemoresistance, while similar effects were not observed for p110 $\delta$ . However, co-targeting of p110 $\alpha$  and p110 $\delta$  led to increased effects on medulloblastoma cell proliferation [15].

Clinical trials have started to evaluate the safety and efficacy of agents targeting this pathway in different brain tumors including medulloblastoma [19]. However, targeting the PI3K pathway remains challenging. Thus, the effort of characterizing the molecular mechanisms and the PI3K downstream effectors in MB will contribute to the elucidation of how PI3K drives oncogenic signaling and may lead to the identification of PI3K target genes as novel candidates for targeted therapy in MB.

Here, we performed a genomic study to compare the changes in the global gene expression profiles of medulloblastoma cells caused by RNAi-mediated down-regulation of p110 $\alpha$  or p110 $\delta$ . Among both *PIK3CA* and *PIK3CD* responsive genes, we identified c-Myc as the transcription factor, whose network of genes was mostly deregulated. Intriguingly, the c-Myc

network included the  $\alpha$ -subunit of the receptor for the leukemia inhibitory factor (LIFR $\alpha$ ). Our data describe, for the first time, a signaling network in which c-Myc controls the expression of LIFR $\alpha$ , in part through the regulation of miR-125b, to contribute to oncogenic p110 $\alpha$  signaling in medulloblastoma.

## Materials and Methods

### Cell culture and treatments

The MB cell lines were obtained and cultured as described in [15], the stable clones DAOY V11 (empty vector transfected) and DAOY M2.1 (*MYC* vector transfected) were described in [24, 25]. PFSK and PNET5 medulloblastoma cell lines were purchased from the American Type Culture Collection and were grown in RPMI 1640 with 10% FCS and penicillin/streptomycin/L-glutamine (Sigma, Buchs, Switzerland). D341 and D458 were a kind gift of Dr. Henry Friedman (Duke University, Durham, NC) [26] and were cultured in Improved MEM medium (Invitrogen, Carlsbad, CA, USA) supplemented with 1% L-glutamine, 1% Penicillin/Streptomycin, 10% FCS. The UW228 cells expressing tamoxifen-inducible c-Myc-ER were kindly provided by Prof. Annie Huang, Hospital for Sick Children, Toronto, Canada and described in [27]. All cells were grown in a humidified atmosphere at 37° and 5% CO<sub>2</sub>. Tamoxifen (Sigma) was used to induce c-Myc expression in these clones. The PI3K inhibitors PIK75 and YM024 (Calbiochem, Darmstadt, Germany) were dissolved in DMSO (Sigma) at 10 mM and diluted to the indicated concentrations in cell culture medium just before use. The Anti-human LIFR $\alpha$  antibody (AF-249-NA) and the recombinant rh-LIF R $\alpha$  (7487-LR) were purchased from R&D Systems (Minneapolis, MN, USA) and were diluted directly into the medium immediately before use. For growth factor stimulations, cells were grown to confluence, starved overnight in culture medium containing 1% FCS. Cells were maintained in serum-free RPMI for 1 h and were then stimulated with LIF (Sigma, Buchs, Switzerland) for 10 min.

### RNA interference and miRNA transfection

MB cell lines were transfected with siRNA pools, each comprising four individual oligonucleotides (SMARTpool small interfering RNA reagents; Dharmacon, Waltham, MA, USA), directed against *PIK3CA* (M-003018-0), *PIK3CD* (M-006775-02-0005), *MYC* (M-003282-07), *LIFR* (M-008017-01-0005) using Lipofectamine 2000 (Invitrogen, Carlsbad, CA, USA) as directed by the manufacturer for adherent cell lines. siCONTROL Non-targeting siRNA Pool (D-001206-14-20) (Dharmacon) composed of four siCONTROL Non-targeting siRNAs was used as negative control. All siRNAs were used at a final concentration of 20 nM. Cells were incubated for 24 h to 48 h and after mRNA and protein were extracted to assess protein expression by Western blotting and mRNA expression by TaqMan analysis.

DAOY cells were transfected with 20nM of miRIDAN hairpin inhibitor directed against mature hsa-miR-125b, 20 nM of precursor for hsa-miR-125b-5p or with Hairpin Negative Control (Thermo Fisher Scientific, Waltham, MA, USA) using SilentFect (Biorad, Hercules, CA, USA) as suggested by the manufacturer. Protein and mRNA were extracted and analyzed after 48h.

### Plasmid transfections

DAOY cells were transfected with expression plasmids using the Lipofectamine Plus reagent (Invitrogen) according to the manufacturer's recommended protocol. The plasmids encoding for activated PI3K-p110 $\alpha$  (*PIK3CA* CAAX) and pcDNA3 (empty vector control) were described in [28].

## Microarray analysis

The cDNA microarray analysis was performed in collaboration with the Functional Genomic Center of the University Zurich, Switzerland. Human Genome-U133 Plus 2.0 Affymetrix GeneChips arrays (Affymetrix, Santa Clara, CA, USA) were used to assess the gene expression data. Raw data generated by the GCOS Software (Affymetrix) were processed by using the RMA method [29] and further statistically analyzed by using the software R and applying Student's t-test.

Each experiment represented a group of three independent biological replicates. Results are expressed as fold change, and differences in expression were considered significant if the fold change was  $> 2.0$  or  $< -2$  and the P-value  $< 0.001$ . Comparative and cluster analysis of the data were performed using the softwares Cluster 3.0 and TreeView [30]. The GeneGO MetaCore (GeneGO, St Joseph, MI, USA) was used to identify affected pathways and networks of genes, according to their ontological categories. The data was deposited in the Gene Expression Omnibus and is accessible through GEO series accession number GSE40564 (<http://www.ncbi.nlm.nih.gov/geo>).

## Gene expression analysis

Total RNA was extracted using the RNeasy Mini Kit (Qiagen, Basel, Switzerland) and converted into cDNA using High-Capacity cDNA Reverse Transcription Kit according to manufacturer's instructions (Applied Biosystems, Foster City, CA, USA). Assays-on-Demand Gene Expression products (Applied Biosystems) were used to measure mRNA expression levels of *PIK3CA* (Hs00907965\_m1), *PIK3CD* (Hs00192399\_m1), *MYC* (Hs00153408\_m1), *LIFR* (Hs00158730\_m1) and *GAPDH* (Hs99999905\_m1; internal control gene). Relative mRNA expression levels were calculated using the comparative threshold cycle (CT) method.

The miRNAs extraction procedure via RNeasy Mini Kit (Qiagen, Basel, Switzerland) was followed by specific reverse transcription and amplification using hsa-miR-125b (000449) and U6 snRna (001973; loading control). Relative miRNA expression levels were calculated using the comparative threshold cycle (CT) method.

For semi-quantitative analysis of the gene expression, the One-Step RT-PCR Kit (Qiagen) was employed. The primers for *LIF*, *LIFR* and *GAPDH* were purchased from Microsynth (Balgach, Switzerland). DNA was separated on 2.5% agarose gel and stained with GelRed (Biotium, Hayward, CA, USA).

The expression data of medulloblastoma ( $n = 62$ ) which are available from NCBI's Gene Expression Omnibus (<http://www.ncbi.nlm.nih.gov/geo/>; accession number GSE10327) published by Kool et al., [31] and expression data of a second cohort of medulloblastoma ( $n = 103$ ; available from NCBI's Gene Expression Omnibus (<http://www.ncbi.nlm.nih.gov/geo/>; accession number GSE21140, reported by Northcott et al. [32]) were used for analysis. Data are accessible through the open access database R2 for visualization and analysis of microarray data (<http://r2.amc.nl>), and data were generated using the R2 microarray analysis and visualization platform (<http://r2.amc.nl>). Gene expression levels were compared using the Kruskal-Wallis test. If this global test was significant, Dunn's post hoc tests were used to compare the groups.

## Western blotting

Cell lysates were prepared in RIPA buffer (50mM Tris-Cl, [pH 6.8], 100mM NaCl, 1% w/v Triton X-100, 0.1% w/v SDS) supplemented with Complete Mini Protease Inhibitor Cocktail (Roche Applied Sciences, Germany) and with the phosphatase inhibitors  $\beta$ -glycerophosphate (20mM) and  $\text{Na}_3\text{VO}_4$  (200 mM). Proteins were separated by SDS-polyacrylamide gel electrophoresis and transferred on hydrophobic polyvinylidene difluoride (PVDF) membrane

(Amersham, GE Healthcare, UK). Antibodies specific for PI3K p110 $\alpha$  (sc-1331), p110 $\delta$  (sc-136032), c-Myc (sc-789), LIFR (sc-659), Akt1/2/3 (sc-8312), ERK 1/2 (sc-99) (Santa Cruz Biotechnology, CA, USA) were diluted 1/500 in 5% BSA, phospho-ERK1/2 (Thr202/Tyr204) (cs-4370), phospho-Akt (Ser473; Thr308) (cs-3787; cs-2965), phospho-S6 (Ser235/236, Ser240/244) (cs-2211; sc-5364) (Cell Signaling Technology, Inc., Danvers, MA, USA),  $\beta$ -actin (Sigma-Aldrich Chemie GmbH, Buchs, Switzerland) (A5441) were diluted 1/1000 in 5% BSA. Chemiluminescence was used for detection using SuperSignal West Femto Maximum Sensitivity Substrate (Thermo Fisher Scientific Inc., Rockford, IL, USA).

## Cell proliferation assays

Cell proliferation was assessed using the Cell Titer 96 Aqueous Cell Proliferation Assay (Promega, Madison, WI, USA). Data are expressed as average values from at least three independent experiments.

## Chicken chorioallantoic membrane assay

Fertilized chicken eggs (*Gallus gallus*) purchased from a local hatchery were incubated in a humidified incubator at 37°C. On embryonic day 3, a squared opening was excised into the shell and sealed with tape. Upon 96h of incubation, a silicon ring was placed on the chorioallantoic membrane and after gentle a scraping, a suspension of 5 million DAOY cells in 20ml phosphate-buffered saline was applied onto the lacerated membrane. On embryonal day 10, the formed tumors were treated with either rh-LIF $\alpha$  (Recombinant Human LIFR $\alpha$ , R&D Systems, Minneapolis, USA, catalog number 7487-LR) or phosphate-buffered saline for 4 consecutive days. On embryonal day 14, tumor volume was measured, as described in [33] and the embryos were sacrificed.

## ChIP-on-chip

ChIP-on-chip experiments using a MYC antibody were performed as previously described [24, 34].

## Ethics statement

All the experiments were performed in conformity with the Swiss animal protection law, requiring no specific approval for working on avian embryos before day 15 of their embryonal development. Thus, on day 14, the experiments were terminated by arterial excision.

## Statistical analysis

All experiments were performed at least in triplicates. Data are represented as mean  $\pm$  SD. The statistical significance of differences between groups was assessed with ANOVA using Tukey's post hoc tests calculated with the statistical software GraphPad PRISM 5 (GraphPad Software, San Diego, CA, USA); P-Values of <0.05 were considered significant and indicated with a single asterisk, a double asterisk if  $P < 0.001$  or a triple asterisk if  $P < 0.001$ . All statistical analyses were intended to be rather exploratory than confirmatory and nominal p-values are reported, without adjustment for multiple testing.

Distribution of gene expression levels were compared using the Kruskal-Wallis test. P-values < 0.05, two-tailed were considered statistically significant. Statistical analyses were performed using GraphPad Prism 4 (GraphPad Software, San Diego, CA, USA).

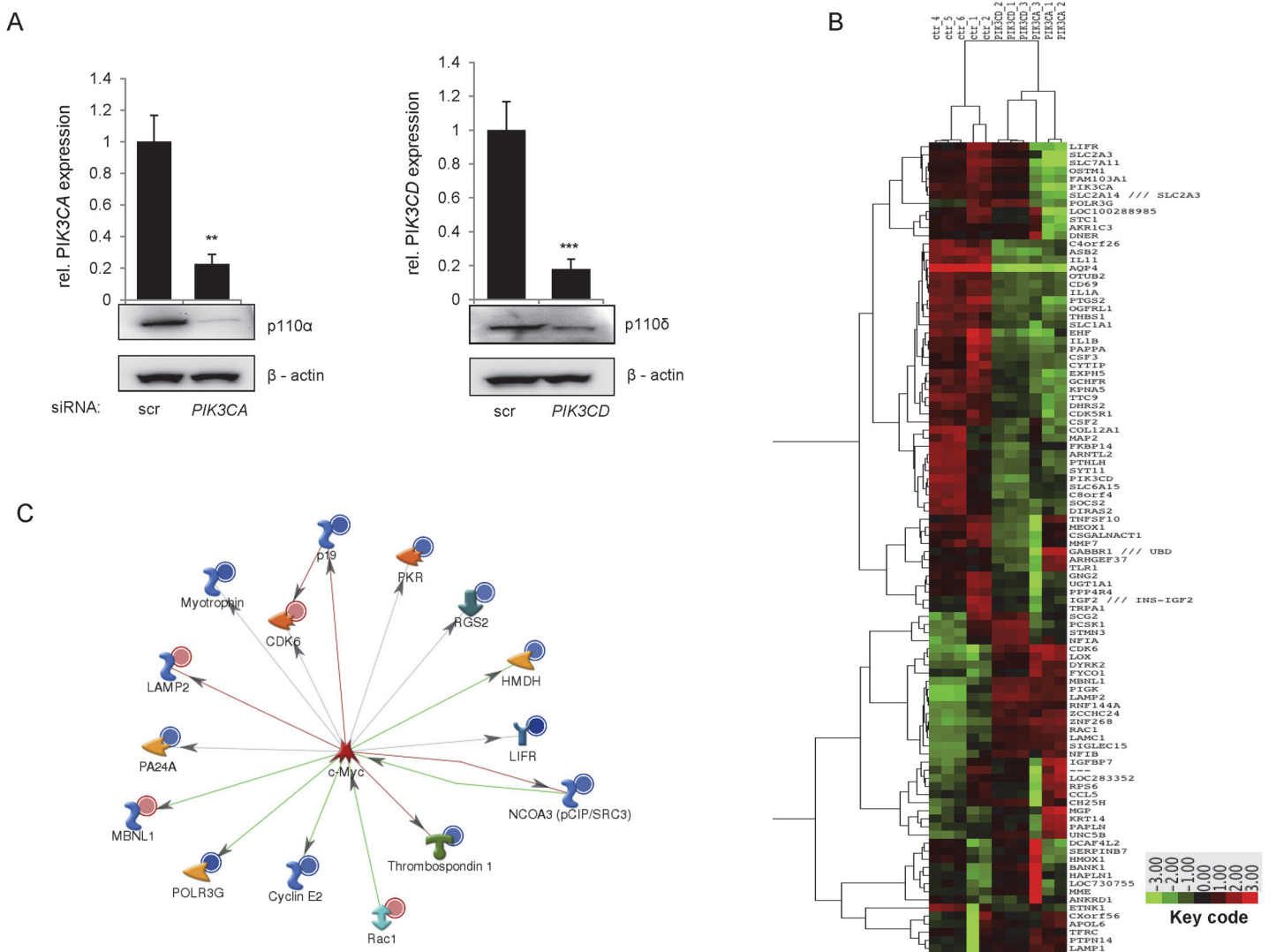


**Fig 1. Gene expression analysis.** (a) DAOY cells were transfected with siRNA against *PIK3CA* or *PIK3CD* and analyzed 48h post transfection for gene down-regulation at mRNA level by real-time PCR and at protein level by Western blot. (b) Heat map representing the expression of *PIK3CA* and *PIK3CD* regulated genes. (c) GeneGo Metacore analysis of transcriptional networks. The set of genes deregulated by *PIK3CA* silencing in DAOY cells were analyzed via GeneGo Metacore software. The most affected network comprising the oncogene *c-Myc* and some its downstream targets is shown.

doi:10.1371/journal.pone.0123958.g001

## Results

### Gene expression analysis reveals selective gene subsets regulated by p110α

In order to investigate how the class I<sub>A</sub> PI3K isoforms p110α and p110δ regulate the expression of specific gene subsets in medulloblastoma, we performed cDNA microarray analysis in DAOY cells transiently transfected with either siRNA targeting p110α, p110δ or control siRNA (Fig 1B). The efficacy of the down-regulation of the target proteins by the respective siRNAs was demonstrated by Western blot analysis, as well as quantitative real time PCR 48h post transfection (Fig 1A). Thus at 48h post transfection, the most efficient target down-regulation was observed and it was therefore chosen for the cDNA microarray analysis. Each experiment was performed in three independent biological replicates, where the results were

normalized to the control values and expressed as fold changes. To define lists of differentially expressed genes, we considered significant those whose fold change was  $> 2.0$  or  $< -2$  and the P-value  $< 0.001$ . Silencing p110 $\alpha$  significantly affected the expression of 453 genes, while silencing p110 $\delta$  resulted in significant changes in 305 genes, showing that p110 $\alpha$  has an overall higher impact on the regulation of global gene expression in MB. In addition, 75 genes were commonly regulated by both p110 $\alpha$  and p110 $\delta$  (S1 and S2 Tables). The resulting sets of differentially expressed genes were further analyzed using different bioinformatics tools, in order to establish functional networks and identify relevant targets for validation.

## Silencing of p110 $\alpha$ perturbs multiple transcriptional networks in medulloblastoma

To gain insight into the transcriptional networks affected by silencing of p110 $\alpha$  and p110 $\delta$  in medulloblastoma cells, we performed a biostatistics analysis of the gene expression data with GeneGO MetaCore. The software was used to define functional annotations for the selected players, thus assigning them to ontologic categories for association with relevant biologic processes and pathways. The transcriptional networks that were most significantly altered by the down-regulation of p110 $\alpha$  and p110 $\delta$  comprised c-Myc, the estrogen receptor (ER), p53 and STAT3 (S3 Table). The transcriptional network involving c-Myc included the LIFR $\alpha$  as a target gene (Fig 1C). LIFR $\alpha$  was found to be more significantly down-regulated in DAOY cells transfected with p110 $\alpha$  siRNA, than in the case of p110 $\delta$  siRNA (Fig 1B and S4 Table), suggesting that it is selectively regulated by p110 $\alpha$ .

Interestingly, STAT3, a downstream target of LIFR was identified as one of the most significantly altered networks (S3 Table). Thus, down-regulation of p110 $\alpha$  perturbs multiple transcriptional networks in medulloblastoma cells, most notably c-Myc, which is potentially involved in controlling LIFR $\alpha$  expression [35].

## PI3K-p110 $\alpha$ dependent regulation of LIFR $\alpha$ expression

In order to validate the LIFR $\alpha$  as a bona fide target of p110 $\alpha$  in medulloblastoma cell lines, we first used quantitative real time PCR and Western blot analysis to confirm the results obtained from the DNA microarrays. Down-regulation of the expression of the LIFR $\alpha$  could indeed be demonstrated at mRNA and protein level upon selective silencing of p110 $\alpha$ , but not p110 $\delta$  (Fig 2A and 2B and S3 Table). We next sought to investigate whether pharmacological inhibition of p110 $\alpha$  also reduced LIFR $\alpha$  expression levels in medulloblastoma cell lines. YM024 and PIK75, two selective p110 $\alpha$  inhibitors effectively reduced the expression levels of the receptor (Fig 2C and Fig 3A). The levels of LIFR $\alpha$  down-regulation achieved by treatment of DAOY with a low dose (5  $\mu$ M) of YM024 were comparable to the response observed upon p110 $\alpha$  silencing by siRNA (Fig 1 and Fig 2A–2C) and upon PIK75 (100 nM) exposure (Fig 3A and 3C). To further confirm these observations, DAOY cells were transiently transfected with active *PIK3CA* coupled with carboxy-terminal farnesylation signal allowing its localization to the membrane. Increase of p110 $\alpha$  induced a post transcriptional up-regulation of LIFR $\alpha$  expression leading to activation of LIFR $\alpha$  downstream target, S6 (Fig 2D, 2E and 2F). Collectively, these results confirm that p110 $\alpha$  controls the expression of the LIFR $\alpha$  in medulloblastoma cell lines.

## Regulation of LIFR by c-Myc downstream of p110 $\alpha$

We next aimed to analyze the mechanism by which p110 $\alpha$  regulates LIFR $\alpha$  expression. According to the analysis of transcriptional networks performed with GeneGo, c-Myc controls a network of genes comprising LIFR $\alpha$  (Fig 1C). To validate this network, we first analyzed the

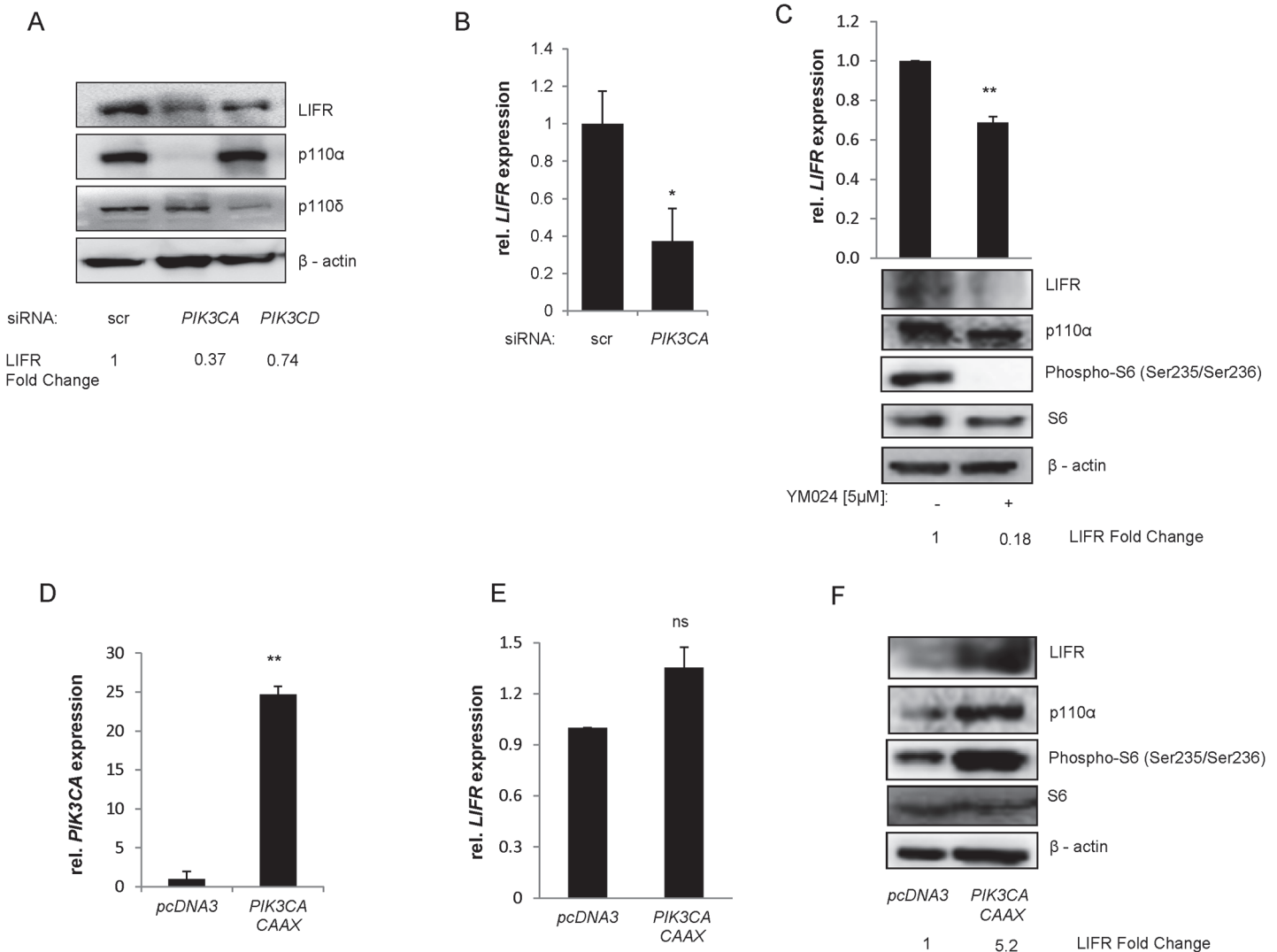


**Fig 2. PI3K-p110α dependent regulation of LIFRα expression.** Expression of LIFRα was analyzed in DAOY cells transfected with siRNA against *PIK3CA* or *PIK3CD* (a), at protein level by Western blot and (b) at mRNA level by RT-PCR after 48h transfection. Protein and mRNA expression of *LIFRα* was also measured upon 24h treatment with YM024 (5 μM). The expression of PI3K-p110α, total and phospho-S6 (Ser235-236) are also shown (c). pcDNA3 vector containing active PI3K-p110α (PIK3CA CAAX) or not were transfected into DAOY cells. 48h post transfection samples were analyzed for p110α and LIFRα expression by qPCR (d-e) or Western blot (f). The expression levels of total and phospho-S6 (Ser240/244) were also measured (c-f). (a, c, f) were quantified by ImageJ analysing software.

doi:10.1371/journal.pone.0123958.g002

expression of LIFRα and c-Myc upon inhibition of p110α with PIK75 in a DAOY-derived cell clone, which over-expresses c-Myc. A strong inhibition of the expression of both proteins was observed upon PI3K inhibitor treatment (Fig 3A). In addition, we used the MB cell line UW228-MycER which expresses a fusion protein comprising c-Myc and the hormone-binding domain of the estrogen receptor (ER) and can be induced by tamoxifen. We observed that LIFRα expression was induced in a time-dependent manner, which paralleled with the induction of c-Myc expression (Fig 3B), previously described as a consequence of general increase in protein synthesis upon tamoxifen treatment [27, 36].

To further investigate p110α —c-Myc-dependent regulation of LIFRα, we performed simultaneous or alternate inhibition of p110α (with PIK75) and induction of c-Myc (with tamoxifen). An impaired c-Myc-dependent rescue of LIFRα protein expression was observed



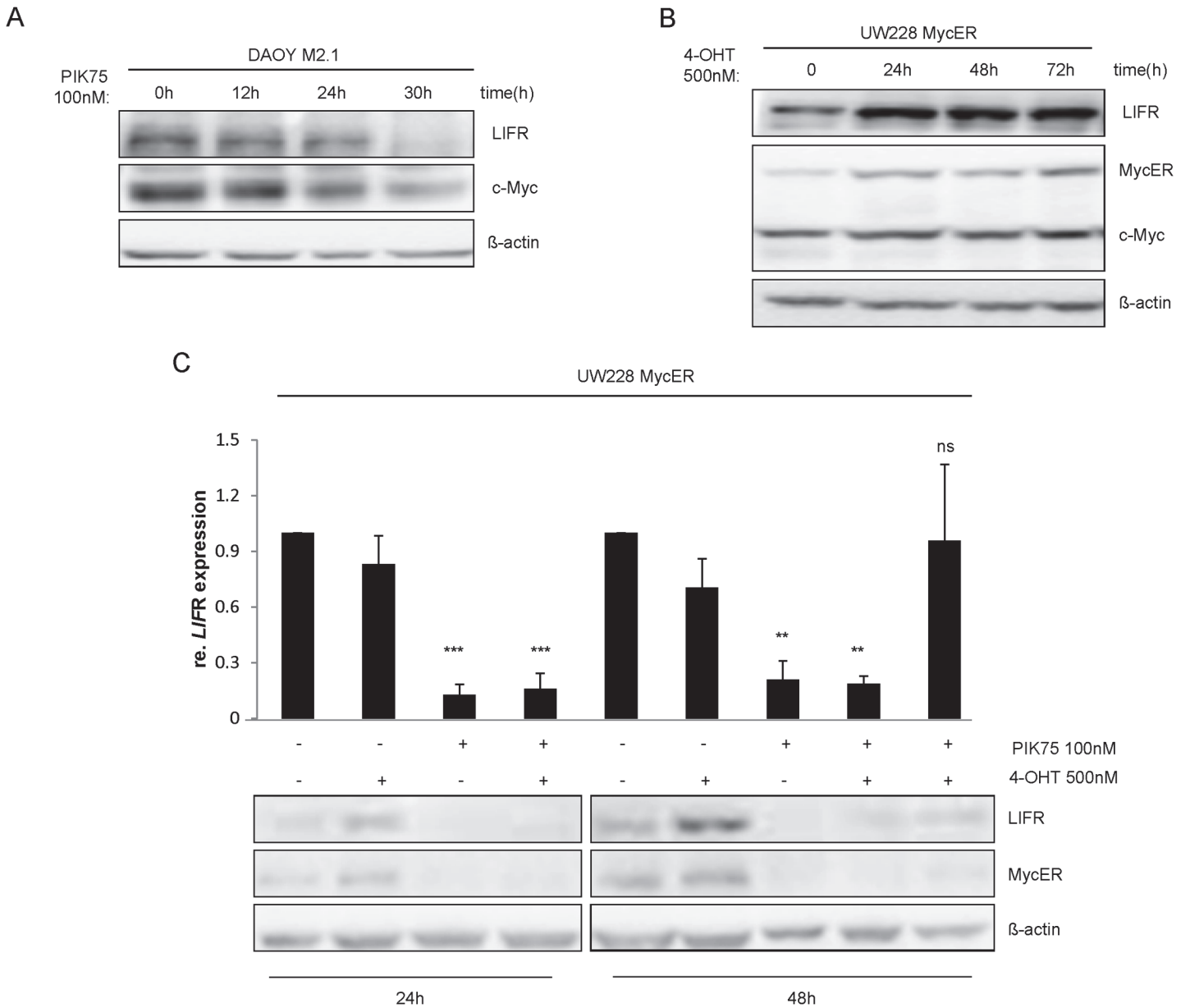


**Fig 3. p110 $\alpha$  regulates LIFR expression through c-Myc.** The protein expression levels of c-Myc and LIFR $\alpha$  were evaluated after 12h, 24h and 30h of 100nM PIK75 exposure by Western blot (a) in DAOY-derived cell clones overexpressing c-Myc (DAOY M2.1) and (b) in UW228-Myc-ER cells induced for c-Myc expression by tamoxifen for 24 h, 48 h and 72 h. (c) LIFR $\alpha$  mRNA levels were analyzed by qPCR and protein levels were analyzed by Western blot in the inducible UW228-Myc-ER cells treated independently, simultaneously or in alternate manner with the p110 $\alpha$  inhibitor PIK75 (100 nM) and/or with tamoxifen (500 nM) for 24 h or 48 h. UW228-Myc-ER were simultaneously exposed to both drugs for 24h (bar 4/lane 4), alternately for 48 h, bar 4/lane 4 24 h tamoxifen (500 nM) exposure followed by 24 h PIK75 (100 nM) and bar 5/lane5 24 h PIK75 (100 nM) treatment followed by 24h tamoxifen (500 nM) induction.

doi:10.1371/journal.pone.0123958.g003

(Fig 3C). Interestingly, at transcriptional level, a partial rescue of the cytokine receptor was observed after 24h of PIK-75 exposure followed by 24h of c-Myc induction (Fig 3C). Together these results confirm the functionality of the gene network identified by bioinformatic analysis and describe a role for c-Myc as a regulator of LIFR $\alpha$  expression in MB cell lines.

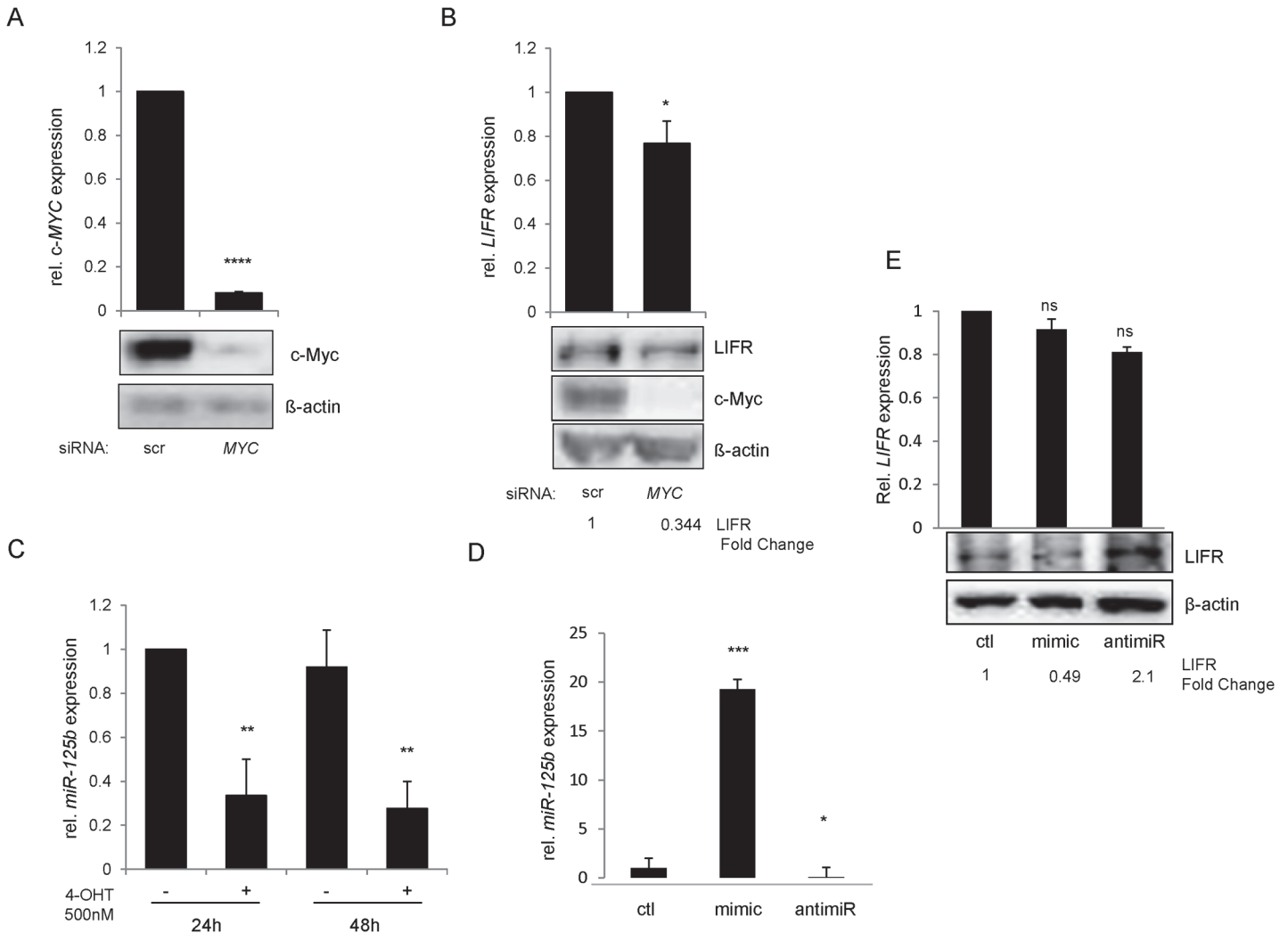


**Fig 4. c-Myc regulates LIFR expression via miR-125b.** Expression of c-Myc (a) and LIFR $\alpha$  (b) were analyzed by qPCR and Western Blot in DAOY M2.1 cells, overexpressing c-Myc, transfected with siRNA against c-Myc. (c) miR-125b expression levels were measured by qPCR after 24h and 48h of 4-OHT treatment in UW228-Myc-ER cells. MiR-125b fold change was calculated via normalization to U6 snRNA expression levels in the corresponding condition (d) miR-125b expression was analyzed by qPCR after transfection with mimic or antagomir for miR-125b in DAOY cells. MiR-125b fold change was calculated as in (c) (e) LIFR $\alpha$  expression level was analyzed by qPCR and Western blot after transfection with mimic or antagomir for miR-125b. (b) and (e) were quantified by ImageJ analysis software.

doi:10.1371/journal.pone.0123958.g004

### c-Myc dependent inhibition of miR-125b controls LIFR $\alpha$ expression

To elucidate the mechanism of the c-Myc-dependent regulation of the LIFR $\alpha$ , we first performed mRNA and protein expression analysis of LIFR $\alpha$  upon c-Myc silencing using the DAOY MB cell line over-expressing the oncogene. Silencing c-Myc induced a decrease in LIFR $\alpha$  protein and mRNA expression level (Fig 4B). Next, we hypothesized whether c-Myc regulates transcriptionally the expression of LIFR $\alpha$  by directly binding to its promoter. Possible binding sites of c-Myc on the LIFR promoter sequence were investigated using the software Genomatix. More than 40 possibilities were found (data not shown), providing a hint that c-Myc may bind to the promoter of LIFR also in medulloblastoma. However, using ChIP-on-chip analysis [24], we were unable to confirm a direct binding of c-Myc to the promoter of the LIFR (data not shown). Since c-Myc is well known miRNA regulator in medulloblastoma [37]

and to this date LIFR $\alpha$  transcriptional regulation is very poorly studied we hypothesized, a c-Myc-dependent indirect control of *LIFR* expression via miRNA. Recent studies have described an auto-regulatory loop connecting the microRNA precursor of the *let-7* family with c-Myc. The oncogene transcriptionally regulates the expression of the *let-7* family members, which in turn regulate c-Myc post-transcriptionally [38]. Using the UW228 medulloblastoma cell line, expressing inducible c-Myc, we could show a significant decrease in miR-125b (a member of the *let-7* family) expression upon c-Myc induction (Fig 4C). Interestingly, another group has recently revealed that miR-125a, a miR-125b homologue, directly binds to the LIFR $\alpha$  3'-UTR and inhibits its protein and mRNA expression [39, 40]. To assess the impact of miR-125b on LIFR $\alpha$  expression, DAOY cells were transiently transfected with the corresponding pre- or anti-miR. mRNA and protein analysis revealed miR-125b-dependent post transcriptional regulation of the receptor (Fig 4E). These results confirm the c-Myc-induced positive loop regulating LIFR $\alpha$  expression via inhibition of miR-125b.

## Expression of LIFR $\alpha$ and LIF in medulloblastoma

Our previous work had documented an over-expression of p110 $\alpha$  in primary medulloblastoma, as well as in medulloblastoma cell lines [15]. Therefore, we hypothesized that the LIFR $\alpha$  may also be over-expressed in primary medulloblastoma. A panel of medulloblastoma lines was screened for LIFR $\alpha$  expression by Western blot analysis, and increased expression of the cytokine receptor was observed in all cell lines when compared to normal brain (Fig 5A). PNET5 and UW228 presented the most increased LIFR $\alpha$  expression level among the MB cell lines. The expression analysis at mRNA level showed that 4 out of 7 cell lines expressed detectable levels of LIFR $\alpha$  mRNA (Fig 5B).

We next sought to investigate whether LIFR $\alpha$  was co-expressed with its ligand LIF in MB cell lines. Three cell lines (DAOY, UW228 and PFSK) co-expressed both the ligand and the receptor (Fig 5A and 5B), indicating the presence of an autocrine loop in a subset of medulloblastoma cell lines.

In order to investigate the clinical relevance of LIFR $\alpha$ , its expression was also analyzed in the cancer microarray database Oncomine [41]. Data obtained from a published study by Pomeroy et al. [42] which compared gene expression profiles of different cohorts of classic and desmoplastic medulloblastomas, supratentorial primitive neuroectodermal tumor, atypical teratoid/rhabdoid tumor and glioblastoma vs. normal cerebellum, showed that the *LIFR* was over-expressed in classic medulloblastoma, desmoplastic medulloblastoma and in glioblastoma when compared to normal cerebellum. (S1 Fig).

Next, we investigated the expression levels of *PIK3CA* and *LIFR* in two primary medulloblastoma cohorts published by Kool et al. [31] and Northcott et al. [32]. *LIFR* presented lower expression levels in group WNT and Group 3, while in SHH and Group 4 *LIFR* displayed higher expression levels. This unique expression was confirmed in both medulloblastoma cohorts [31, 32]. The non-WNT tumors (group SHH, group 3 and 4) were characterized by highest *PIK3CA* expression in comparison to patients with good prognosis (group WNT) presenting lower *PIK3CA* expression (Fig 4C). *PIK3CA* and *LIFR* expressions correlated exclusively in the WNT and SHH subgroups, lower and higher expression correspondingly (Fig 5C and S2 Fig).

To further investigate the impact of *LIFR* expression in medulloblastoma tumors, we compared two cDNA microarray data performed on heterozygous for Patched receptor mice, expressing wild type or single copy of *TP53* [43, 44]. Interestingly, in the SHH MB mimicking murine model (*PTCH*<sup>-/+</sup>, *TP53*<sup>-/+</sup>), *LIFR* expression was significantly higher, confirming the role of the cytokine receptor in these tumors (Fig 5D and S3 Fig).

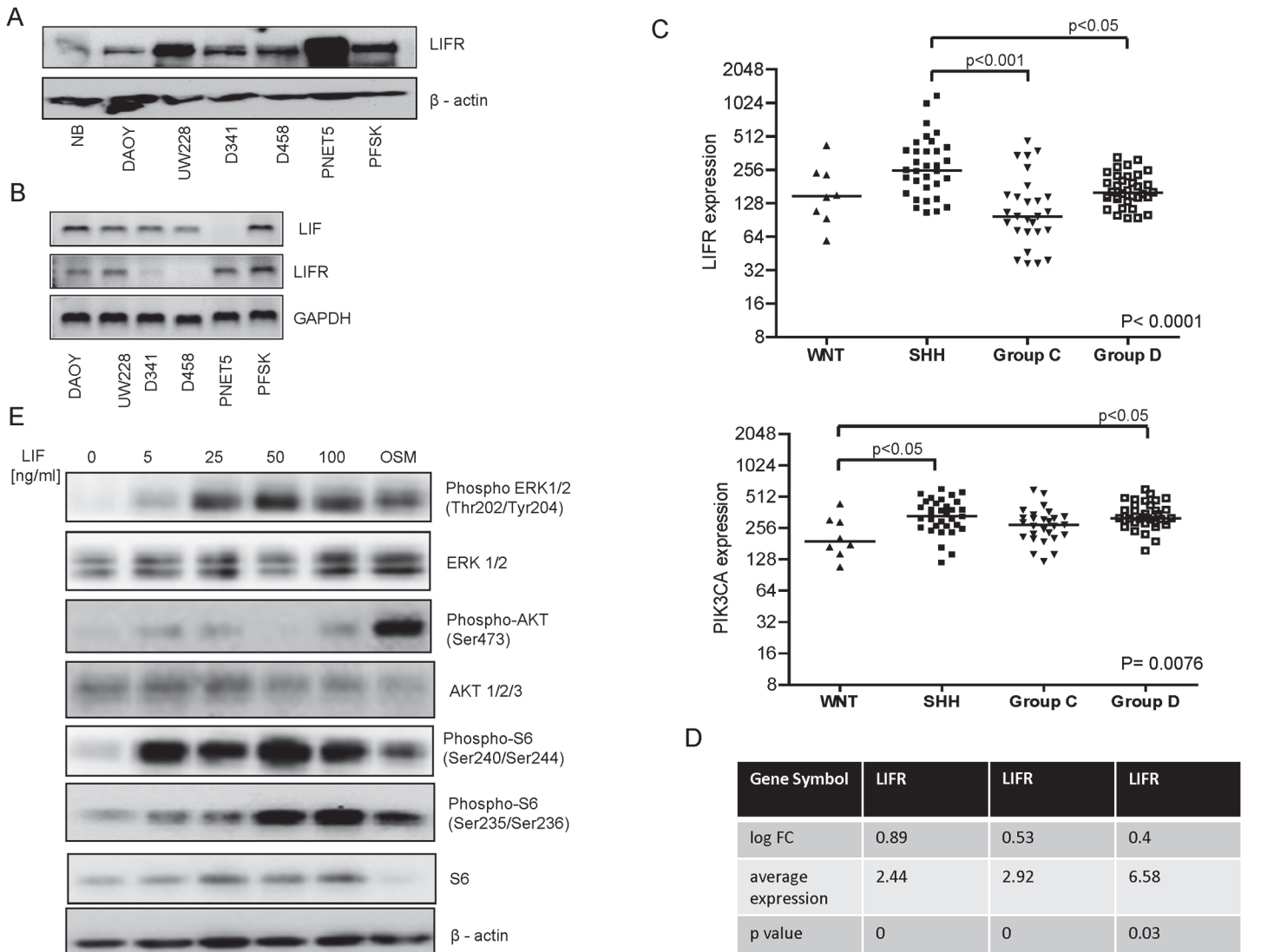


**Fig 5. Expression of LIFR $\alpha$  and LIF in medulloblastoma cell lines and primary brain tumors.** (a) LIFR $\alpha$  protein levels in medulloblastoma cell lines and normal brain (NB) tissue were evaluated by Western blot and compared with  $\beta$ -actin as the loading control. (b) *LIF* and *LIFR* expression in medulloblastoma cell lines was analyzed by semi quantitative RT-PCR. (c) Expression of *PIK3CA* and *LIFR* derived from the transcriptomic analysis of primary medulloblastoma, grouped according to molecular disease variants. Data from Northcott et al [32] are shown. Gene expression levels were compared using the Kruskal-Wallis test and the p-value is shown at the bottom right of the illustration. As this global test was significant, Dunn's post hoc tests were used to compare the groups. P-values < 0,05, as determined by Dunn's post hoc tests, are indicated in order to illustrate the differences. (d) Analysis of cDNA microarray data performed on *PTCH1*<sup>+/-</sup>; *TP53*<sup>+/-</sup> or *PTCH1*<sup>+/-</sup>; *TP53*<sup>+/+</sup> mice. The table represents a summary of fold change (logFC), average expression values (AveExpr), p values obtained by comparison of the two murine strains from Data set GEO accession number GSE37316). (e) Cell lysates of DAOY cells stimulated with or not with 5, 10, 25, 50 and 100 ng/ml of LIF for 10 min were analyzed for expression and phosphorylation of AKT and ERK pathway downstream targets. Treatment of 10 ng/ml of OSM for 10 min was used as a positive control.

doi:10.1371/journal.pone.0123958.g005

### LIFR $\alpha$ activation stimulates multiple intracellular signaling pathways in medulloblastoma

In order to investigate whether the LIFR $\alpha$  is functional in medulloblastoma cell lines, we analyzed the activation status of downstream signaling pathways in response to cell stimulation with LIF. Dose-dependent activation of ERK and AKT pathways, leading to activation via phosphorylation of their downstream target S6 was detected, starting at a concentration of LIF

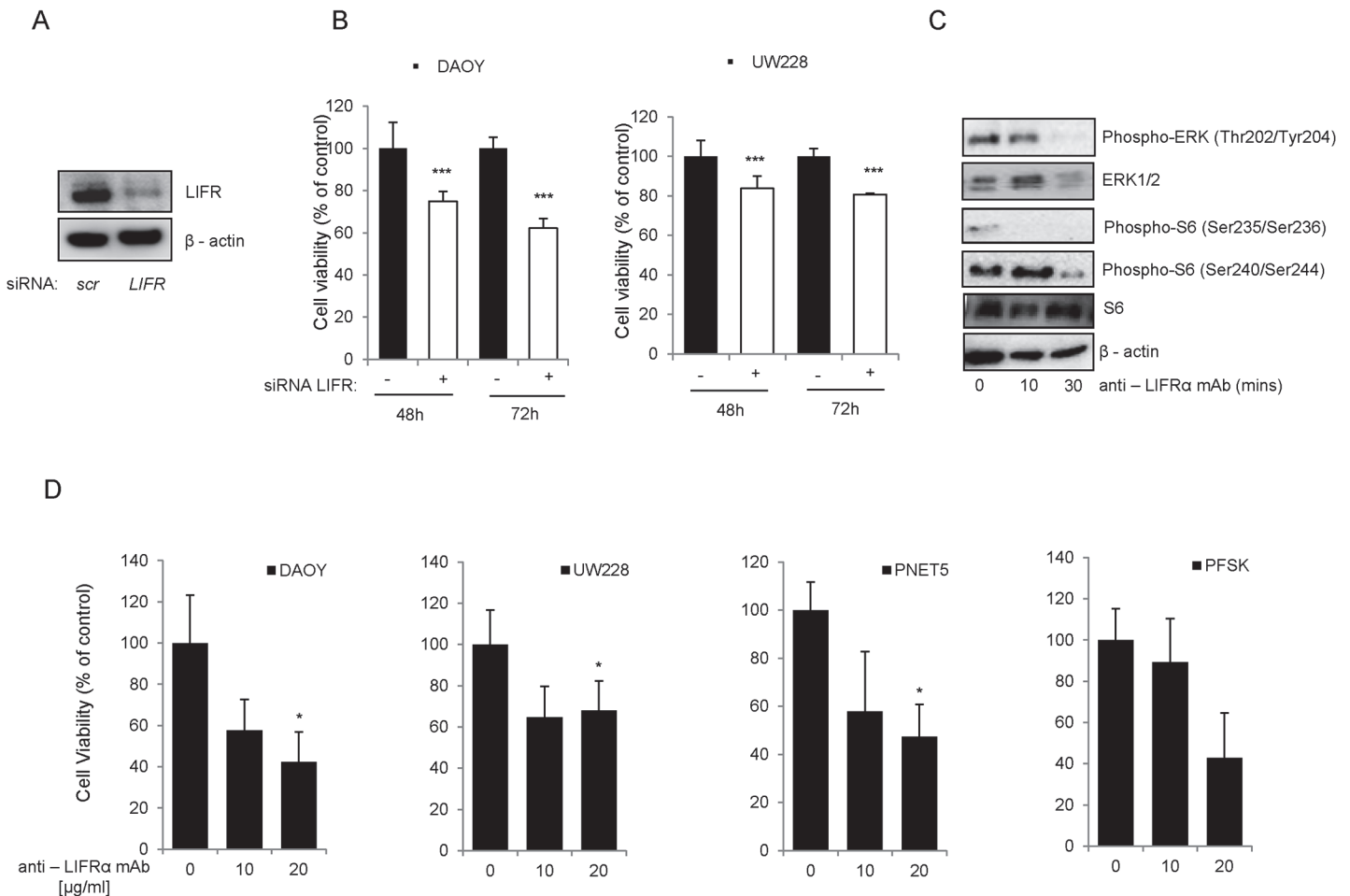


**Fig 6. Effects of LIFR $\alpha$  down-regulation on medulloblastoma cell proliferation and survival.** (a) Protein expression level of LIFR $\alpha$  in DAOY cells transfected with siRNA against *LIFR* compared to the control siRNA transfected cells. (b) The effects on cell viability of the siRNA-mediated target down-regulation of LIFR $\alpha$  (white bars) compared to control siRNA (black bars) in DAOY and UW228 cells was assessed for the indicated time points and expressed as percentages. (c) The protein expression of LIFR $\alpha$  downstream targets was analyzed upon treatment for 10 or 30 min with 20 $\mu$ g/ml of anti-LIFR $\alpha$  neutralizing antibody.  $\beta$ -actin was used as a loading control. (d) Cell viability was evaluated in DAOY, UW228, PNET5 and PFSK cells treated for 48h with an anti-LIFR $\alpha$  neutralizing antibody at the indicated concentrations.

doi:10.1371/journal.pone.0123958.g006

of 5ng/ml and with a maximal effect at 100ng/ml in DAOY cells (Fig 5E). Furthermore, activation of downstream signaling pathways in response to cell stimulation with oncostatin M (OSM), a potent activator of LIFR signaling confirmed our data (Fig 5E and S4 Fig). In view of the activation of these classical downstream signaling pathways, it can be concluded that the LIFR $\alpha$  is indeed functional in medulloblastoma cell lines.

### Targeting LIFR $\alpha$ signaling in medulloblastoma

The role of LIFR $\alpha$  in the control of medulloblastoma cell proliferation and survival was investigated by RNAi downregulation and pharmacological inhibition with a neutralizing antibody against the receptor and subsequent analysis of MB cell responses. We first used siRNA to transiently down-regulate the expression of the LIFR $\alpha$  in medulloblastoma cell lines (Fig 6A).

Down-regulation of the cytokine receptor led to significantly decreased cell proliferation in DAOY and UW228 cell lines (Fig 6B).

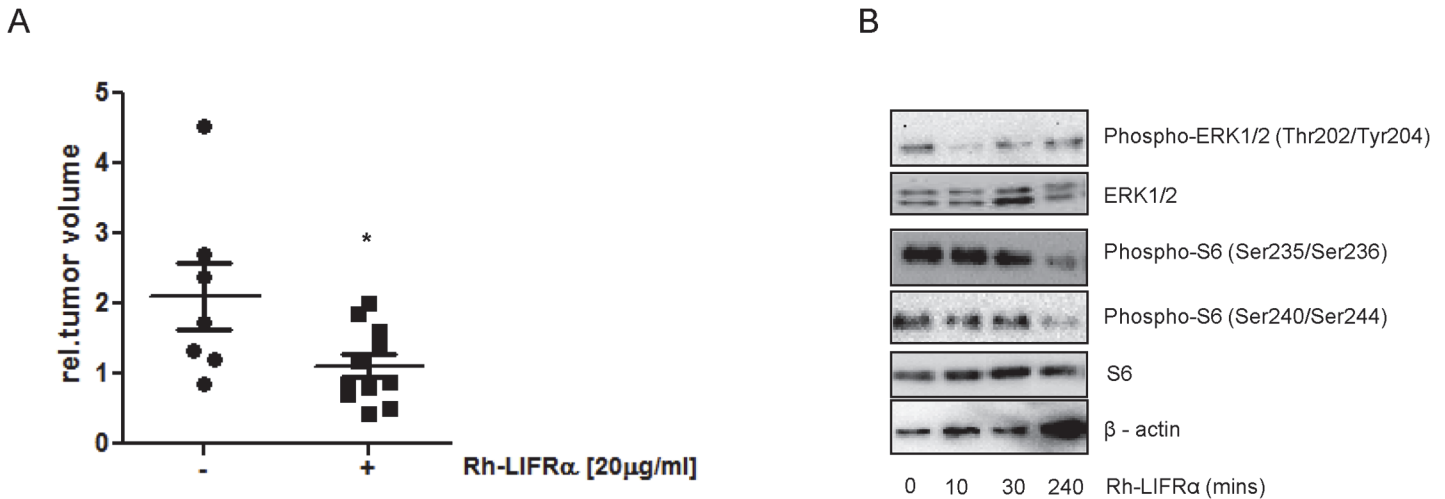


**Fig 7. LIFR $\alpha$  inhibition induces reduction in Medulloblastoma tumor volume.** (a) Tumors formed on (CAM) were treated with 20µg/ml of rh-LIFR $\alpha$  recombinant or phosphate-buffered saline for 4 consecutive days. Quantification of tumor volume changes before and after treatment is shown. Lines indicate the mean of each group, \*P<0.05 compared with control treatment. (b) The expression of LIFR $\alpha$  downstream targets was analyzed upon treatment for 10, 30, 240 min with 20 µg/ml of rh-LIFR $\alpha$ .  $\beta$ -actin was used as a loading control.

doi:10.1371/journal.pone.0123958.g007

Furthermore, we analyzed the effect of the cytokine receptor inhibition on the downstream targets of the signaling pathway. Time-dependent inhibition of ERK and AKT pathways, leading to decreased phosphorylation of their downstream target the ribosomal protein S6, was measured upon treatment of 20µg/ml of LIFR $\alpha$  neutralizing antibody in DAOY cells (Fig 6C). This indicates that the neutralizing antibody disrupts LIF/LIFR $\alpha$  signaling. Similar results were obtained when using a recombinant human soluble LIFR $\alpha$  as a neutralizing reagent (Fig 7B). These results were confirmed in 4 MB cell lines, where upon exposure to LIFR $\alpha$  neutralizing antibody, a significant decrease in cell proliferation was observed (Fig 6D).

In order to explore the therapeutic potential of LIFR $\alpha$  inhibition *in vivo*, we performed a chicken embryo chorioallantoic membrane assay (CAM). Direct application of DAOY cells onto the chorioallantoic membrane led to the formation of solid tumors within 3 days. For the following 4 days, the tumors were treated with 20µg/mL of recombinant human soluble LIFR $\alpha$  as a neutralizing reagent (ligand trap) and their volume was compared to a control treatment. As expected, a significant reduction in the tumor volume was observed upon inhibition of LIF/LIFR $\alpha$  (Fig 7A). Confirmation of the efficacy of the recombinant human soluble LIFR $\alpha$ , was observed in DAOY cells treated for 10, 30 and 240 minutes with 20µg/mL of the neutralizing reagent. As expected, similarly to LIFR $\alpha$  neutralizing antibody, the recombinant human LIFR $\alpha$  inhibited the AKT and ERK pathways leading to decreased phosphorylation of the ribosomal protein S6 (Fig 7B). Together these findings confirm the key involvement of LIFR $\alpha$  in medulloblastoma tumorigenesis.

## Discussion

The PI3K/Akt pathway has been demonstrated to play a key role in medulloblastoma cell proliferation, survival, chemoresistance and migration [4, 11, 15, 16, 45, 46]. Mutations in *PIK3CA* were reported in primary medulloblastoma [23], as well as increased expression of *PIK3CA* at the mRNA and protein level [15]. Isoform-specific or broad specificity PI3K inhibitors have shown anti-tumor activity in medulloblastoma models *in vitro* and *in vivo* [4, 15, 16]. In general, these agents reduced the activation status of classical PI3K downstream targets, such as Akt, mTOR, S6K or GSK-3 $\beta$ .

Targeting p110 $\alpha$  by RNAi or isoform-specific inhibitors had more pronounced effects on medulloblastoma cell responses than in the case of p110 $\beta$  or p110 $\delta$ , indicating a selective role for p110 $\alpha$  in medulloblastoma [15]. This hypothesis was also confirmed by the observation that *PIK3CA* was over-expressed in primary medulloblastoma, compared to normal cerebellum, which was not the case for *PIK3CB* or *PIK3CD* [15]. We have previously shown that while p110 $\delta$  knock-down by siRNA does not impair cell proliferation in MB, co-targeting p110 $\alpha$  and p110 $\delta$  led to a greater reduction cell proliferation than single p110 $\alpha$  targeting [15]. The precise role of p110 $\delta$  in MB however remains to be clarified.

In view of these observations, we hypothesized that p110 $\alpha$  may control the expression of a selective subset of genes implicated in medulloblastoma cell proliferation and/or survival. The comparative DNA microarray analysis of medulloblastoma cell lines in which either p110 $\alpha$  or p110 $\delta$  were down-regulated by siRNA identified such a gene subset.

The LIFR $\alpha$  was validated as a downstream target of p110 $\alpha$  by a combination of approaches, including pharmacological inhibition or over-expression of the class I<sub>A</sub> PI3K isoform. The observation that LIFR $\alpha$  expression was elevated in the SHH subgroup of primary medulloblastoma, further supports this model, in view of the over-expression of *PIK3CA* in this subtype.

Importantly, the LIFR $\alpha$  was shown to be functional in medulloblastoma cell lines, since its activation stimulated classical downstream signaling pathways, such as JAK/STAT, Erk1/2 and PI3K/Akt. Moreover, the observation that medulloblastoma cell lines generally express LIF confirms the presence of an autocrine loop in this malignant brain tumor [47]. LIF is a pleiotropic cytokine, which can sustain proliferation or differentiation depending on cell type or maturation [48]. Deregulated LIF secretion has also been previously described in human cancer, such as breast cancer, rhabdomyosarcoma and medulloblastoma [47, 49, 50]. In medulloblastoma, cell lines, LIF expression was reported to be regulated by p53 [51]. Interestingly, we have shown a p53-dependent negative regulation of the receptor expression in *PTCH*<sup>-/+</sup> mice expressing wild type *TP53* compared to mice expressing heterozygous *TP53*. Considering the previously published LIF dependent negative feedback loop on LIFR $\alpha$  expression [52], the ensemble of these data strongly suggest an indirect p53-dependent regulation of LIFR $\alpha$  via LIF.

To our knowledge, we performed for the first time *in vivo* inhibition of LIFR $\alpha$  which led to tumor volume reduction in CAM assay model. Targeting the LIFR $\alpha$  downstream signaling has also been evaluated in medulloblastoma. Interfering with STAT3 by using a non-peptide small molecule STAT3 inhibitor was reported to decrease cell viability and induce apoptosis in medulloblastoma [39]. A study using resveratrol also reported on the importance of STAT3 signaling in maintenance and survival of medulloblastoma cells [53].

There exist so far few reports on the regulation of LIFR $\alpha$  expression and promoter activity. In breast cancer, c-Myc was shown to act as a negative regulator of LIFR $\alpha$  expression [35]. In MB, we failed to detect a direct binding of c-Myc to the promoter of the receptor. Nevertheless, c-Myc-dependent, multiple-partners transcriptional regulation of LIFR $\alpha$  remains plausible. However, our data support a model in which c-Myc indirectly controls LIFR $\alpha$  protein expression by repressing miR-125b, a negative regulator of the cytokine receptor. In this regard, recent studies have revealed down-regulation of miR-125b in primary medulloblastoma tumors compared to normal fetal brain [54]. Furthermore, the LIFR $\alpha$ -dependent proliferation increase in our MB cell lines, tumor volume reduction upon LIFR $\alpha$  inhibition *in vivo* and the high LIFR $\alpha$  expression levels in the SHH subgroup of MB, are supported by data published by Ferretti et al. [55] documenting miR-125b-dependent inhibition of cerebellar progenitor proliferation, via negative regulation of *Smoothed*, an upstream component in the SHH pathway. Interestingly, data from Peng et al have described the microRNA as prognosis biomarker in oral cavity squamous cell carcinoma [56] suggesting strongly the measurement of the circulating miR-125b also in medulloblastoma. Furthermore, our results suggest PI3K-dependent

transcriptional regulation of LIFR independently of Myc. Up to date, there are no data describing direct interaction between the cytokine receptor promoter and a transcription factor.

Previous studies have reported on cross-talks between the PI3K/Akt pathway and *myc*-family genes. GSK-3 $\beta$  (glycogen synthase kinase 3, isoform  $\beta$ ), which is directly regulated by phosphorylation through Akt controls Myc phosphorylation and stability [12, 57]. An additional mechanism of PI3K-dependent regulation of Myc is through PDK1 (Phosphoinositide-dependent kinase-1). The latter phosphorylates PLK1 (Polo-like kinase 1) which in turn induces MYC phosphorylation at Ser62 and promotes cell growth and survival [58]. In Medulloblastoma, treatment with the PDK1 inhibitor OSU03012 induced apoptosis *in vitro* and inhibited xenograft tumor growth [4].

In embryonal tumors, including medulloblastoma, targeting the AKT and ERK pathways using a quassinoid analogue induced c-Myc and N-myc down-regulation [7, 59]. Inhibition of PI3K using a selective inhibitor was also reported to induce N-myc down-regulation in neuroblastoma [60]. N-myc was shown to play an important role in the regulation of PI3K-mediated VEGF secretion in neuroblastoma cells [61, 62]. Interestingly, *MYCN* is often found amplified in SHH type of Medulloblastoma and its expression is linked to poor patient outcome [5, 63]. Recently, *MYC* amplification has been reported to be implicated in the resistance of tumors with activated *PIK3CA* to pharmacological inhibitors of p110 $\alpha$  [40, 64].

Together our results delineate a novel signaling pathway from p110 $\alpha$  to c-Myc, mir-125b and LIFR $\alpha$ , which contributes to key medulloblastoma cell responses and may be further studied to develop novel targeted therapies for this common and devastating childhood malignancy.

## Supporting Information

**S1 Fig. LIFR expression in primary brain tumors.** *LIFR* gene expression profile in different cohorts of atypical teratoid/rhabdoid tumour (1), classic (2) and desmoplastic (3) medulloblastomas, glioblastoma (4) and primitive neuroectodermal tumor (5) compared to normal cerebellum (0). Due to large variations in sample sizes, statistical analysis was not performed. The fold changes (FC) in expression are listed as a reference for this analysis (FC<sub>Malignant Glioma</sub> = 1.53, FC<sub>Desmoplastic Medulloblastoma</sub> = 1.3, FC<sub>Classic Medulloblastoma</sub> = 1.19, FC<sub>AT/RT</sub> = -1.8). Data were analyzed with [www.oncomine.org](http://www.oncomine.org), based on Pomeroy et al (27). (TIF)

**S2 Fig. Expression of LIFR and PIK3CA in primary medulloblastoma subtypes.** Expression of *PIK3CA* and *LIFR* derived from the transcriptomic analysis of primary medulloblastoma, grouped according to molecular disease variants. Data from Kool et al. (28) are shown. (TIFF)

**S3 Fig. LIFR $\alpha$  expression in mouse-driven model of SHH medulloblastoma.** Microarray analysis of LIFR $\alpha$  expression in murine PTCH $\pm$ - p53 $\pm$ - cancer stem cells compared to PTCH $\pm$ - p53 $\pm$  cells (Data set GEO accession number GSE37316). Volcano plot of fold changes (log<sub>2</sub> scale) versus p values (-log<sub>10</sub> scale, grey) and adjusted p values (-log<sub>10</sub> scale, pink) is shown. Highlighted in red are the values for various probe sets representing LIFR. (TIF)

**S4 Fig. LIFR $\alpha$  signaling in medulloblastoma.** Cell lysates of DAOY cells stimulated with oncostatin M (OSM) for 10 min were analyzed for expression and phosphorylation of the indicated OSM downstream targets. (TIFF)



**S1 Table. List of PI3K-p110 $\alpha$  regulated genes in DAOY cells.** List of a gene set deregulated upon *PIK3CA* silencing in DAOY cells.

(TIFF)

**S2 Table. List of PI3K-p110 $\delta$  regulated genes in DAOY cells.** List of a gene set deregulated upon *PIK3CD* silencing in DAOY cells.

(TIFF)

**S3 Table. Analysis of transcriptional networks by GeneGo Metacore.** Hit list of the transcription factors whose gene networks were mostly affected by the RNAi mediated downregulation of *PIK3CA* and *PIK3CD* in DAOY cells.

(TIF)

**S4 Table. Genes involved in c-Myc transcriptional network.** Fold changes in the gene expression of predicted c-Myc target genes in DAOY cells transfected with the indicated siRNAs (targeting *PIK3CA* or *PIK3CD*) versus control siRNA are listed.

(TIFF)

## Acknowledgments

Valeriya Dimitrova and Paulina Ćwiek are members of the Graduate School of Cellular and Biomedical Science of University of Bern. We thank Prof. Annie Huang, Hospital for Sick Children, Toronto, Canada for providing UW-228 MycER cells. We thank Marianeve Quartuccio for technical assistance.

## Author Contributions

Conceived and designed the experiments: AA FS V. Dimitrova. Performed the experiments: FS V. Dimitrova AOVB HR PC PA. Analyzed the data: FS V. Dimitrova AOVB HR PC PA. Contributed reagents/materials/analysis tools: V. Djonov PA. Wrote the paper: FS V. Dimitrova PA AA.

## References

1. Wechsler-Reya R, Scott MP. The developmental biology of brain tumors. *Annu Rev Neurosci.* 2001; 24:385–428. PMID: [11283316](#)
2. Massimino M, Giangaspero F, Garre ML, Gandola L, Poggi G, Biassoni V, et al. Childhood medulloblastoma. *Crit Rev Oncol Hematol.* 2011 Jul; 79(1):65–83. doi: [10.1016/j.critrevonc.2010.07.010](#) PMID: [21129995](#)
3. Gilbertson R. Paediatric embryonic brain tumours. biological and clinical relevance of molecular genetic abnormalities. *Eur J Cancer.* 2002 Mar; 38(5):675–85. PMID: [11916550](#)
4. Baryawno N, Sveinbjornsson B, Eksborg S, Chen CS, Kogner P, Johnsen JI. Small-molecule inhibitors of phosphatidylinositol 3-kinase/Akt signaling inhibit Wnt/beta-catenin pathway cross-talk and suppress medulloblastoma growth. *Cancer Res.* 2010 Jan 1; 70(1):266–76. doi: [10.1158/0008-5472.CAN-09-0578](#) PMID: [20028853](#)
5. Kool M, Korshunov A, Remke M, Jones DT, Schlanstein M, Northcott PA, et al. Molecular subgroups of medulloblastoma: an international meta-analysis of transcriptome, genetic aberrations, and clinical data of WNT, SHH, Group 3, and Group 4 medulloblastomas. *Acta Neuropathol.* 2012 Apr; 123(4):473–84. doi: [10.1007/s00401-012-0958-8](#) PMID: [22358457](#)
6. Grotzer MA, Castelletti D, Fiaschetti G, Shalaby T, Arcaro A. Targeting Myc in pediatric malignancies of the central and peripheral nervous system. *Curr Cancer Drug Targets.* 2009 Mar; 9(2):176–88. PMID: [19275758](#)
7. Castelletti D, Fiaschetti G, Di Dato V, Ziegler U, Kumps C, De Preter K, et al. The quassinoid derivative NBT-272 targets both the AKT and ERK signaling pathways in embryonal tumors. *Mol Cancer Ther.* 2010 Dec; 9(12):3145–57. doi: [10.1158/1535-7163.MCT-10-0539](#) PMID: [20889731](#)

8. von Bueren AO, Shalaby T, Oehler-Janne C, Arnold L, Stearns D, Eberhart CG, et al. RNA interference-mediated c-MYC inhibition prevents cell growth and decreases sensitivity to radio- and chemotherapy in childhood medulloblastoma cells. *BMC Cancer*. 2009; 9(10). doi: [10.1186/1471-2407-9-10](https://doi.org/10.1186/1471-2407-9-10) PMID: [19134217](https://pubmed.ncbi.nlm.nih.gov/19134217/)
9. Henssen A, Thor T, Odersky A, Heukamp L, El-Hindy N, Beckers A, et al. BET bromodomain protein inhibition is a therapeutic option for medulloblastoma. *Oncotarget*. 2013 Nov; 4(11):2080–95. PMID: [24231268](https://pubmed.ncbi.nlm.nih.gov/24231268/)
10. Bandopadhyay P, Bergthold G, Nguyen B, Schubert S, Gholamin S, Tang Y, et al. BET bromodomain inhibition of MYC-amplified medulloblastoma. *Clin Cancer Res*. 2014 Feb 15; 20(4):912–25. doi: [10.1158/1078-0432.CCR-13-2281](https://doi.org/10.1158/1078-0432.CCR-13-2281) PMID: [24297863](https://pubmed.ncbi.nlm.nih.gov/24297863/)
11. Morfouace M, Shelat A, Jacus M, Freeman BB 3rd, Turner D, Robinson S, et al. Pemetrexed and gemcitabine as combination therapy for the treatment of Group3 medulloblastoma. *Cancer Cell*. 2014 Apr 14; 25(4):516–29. doi: [10.1016/j.ccr.2014.02.009](https://doi.org/10.1016/j.ccr.2014.02.009) PMID: [24684846](https://pubmed.ncbi.nlm.nih.gov/24684846/)
12. Kenney AM, Widlund HR, Rowitch DH. Hedgehog and PI-3 kinase signaling converge on Nmyc1 to promote cell cycle progression in cerebellar neuronal precursors. *Development*. 2004 Jan; 131(1):217–28. PMID: [14660435](https://pubmed.ncbi.nlm.nih.gov/14660435/)
13. Hernan R, Fasheh R, Calabrese C, Frank AJ, Maclean KH, Allard D, et al. ERBB2 up-regulates S100A4 and several other prometastatic genes in medulloblastoma. *Cancer Res*. 2003 Jan 1; 63(1):140–8. PMID: [12517790](https://pubmed.ncbi.nlm.nih.gov/12517790/)
14. Del Valle L, Enam S, Lassak A, Wang JY, Croul S, Khalili K, et al. Insulin-like growth factor I receptor activity in human medulloblastomas. *Clin Cancer Res*. 2002 Jun; 8(6):1822–30. PMID: [12060623](https://pubmed.ncbi.nlm.nih.gov/12060623/)
15. Guerreiro AS, Fattet S, Fischer B, Shalaby T, Jackson SP, Schoenwaelder SM, et al. Targeting the PI3K p110alpha isoform inhibits medulloblastoma proliferation, chemoresistance, and migration. *Clin Cancer Res*. 2008 Nov 1; 14(21):6761–9. doi: [10.1158/1078-0432.CCR-08-0385](https://doi.org/10.1158/1078-0432.CCR-08-0385) PMID: [18980969](https://pubmed.ncbi.nlm.nih.gov/18980969/)
16. Guerreiro AS, Fattet S, Kulesza DW, Atamer A, Elsing AN, Shalaby T, et al. A sensitized RNA interference screen identifies a novel role for the PI3K p110gamma isoform in medulloblastoma cell proliferation and chemoresistance. *Mol Cancer Res*. 2011 Jul; 9(7):925–35. doi: [10.1158/1541-7786.MCR-10-0200](https://doi.org/10.1158/1541-7786.MCR-10-0200) PMID: [21652733](https://pubmed.ncbi.nlm.nih.gov/21652733/)
17. Reynolds CP, Kang MH, Carol H, Lock R, Gorlick R, Kolb EA, et al. Initial testing (stage 1) of the phosphatidylinositol 3' kinase inhibitor, SAR245408 (XL147) by the pediatric preclinical testing program. *Pediatr Blood Cancer*. 2012 Sep 21.
18. Pocza T, Sebestyen A, Turanyi E, Krenacs T, Mark A, Sticz TB, et al. mTOR Pathway As a Potential Target In a Subset of Human Medulloblastoma. *Pathol Oncol Res*. 2014 Apr 16.
19. Holand K, Salm F, Arcaro A. The phosphoinositide 3-kinase signaling pathway as a therapeutic target in grade IV brain tumors. *Curr Cancer Drug Targets*. 2011 Oct; 11(8):894–918. PMID: [21861842](https://pubmed.ncbi.nlm.nih.gov/21861842/)
20. Arcaro A, Guerreiro AS. The phosphoinositide 3-kinase pathway in human cancer: genetic alterations and therapeutic implications. *Curr Genomics*. 2007 Aug; 8(5):271–306. doi: [10.2174/138920207782446160](https://doi.org/10.2174/138920207782446160) PMID: [19384426](https://pubmed.ncbi.nlm.nih.gov/19384426/)
21. Engelman JA. Targeting PI3K signalling in cancer: opportunities, challenges and limitations. *Nat Rev Cancer*. 2009 Aug; 9(8):550–62. doi: [10.1038/nrc2664](https://doi.org/10.1038/nrc2664) PMID: [19629070](https://pubmed.ncbi.nlm.nih.gov/19629070/)
22. Liu P, Cheng H, Roberts TM, Zhao JJ. Targeting the phosphoinositide 3-kinase pathway in cancer. *Nat Rev Drug Discov*. 2009 Aug; 8(8):627–44. doi: [10.1038/nrd2926](https://doi.org/10.1038/nrd2926) PMID: [19644473](https://pubmed.ncbi.nlm.nih.gov/19644473/)
23. Broderick DK, Di C, Parrett TJ, Samuels YR, Cummins JM, McLendon RE, et al. Mutations of PIK3CA in anaplastic oligodendrogliomas, high-grade astrocytomas, and medulloblastomas. *Cancer Res*. 2004 Aug 1; 64(15):5048–50. PMID: [15289301](https://pubmed.ncbi.nlm.nih.gov/15289301/)
24. Fiaschetti G, Castelletti D, Zoller S, Schramm A, Schroeder C, Nagaishi M, et al. Bone morphogenetic protein-7 is a MYC target with prosurvival functions in childhood medulloblastoma. *Oncogene*. 2011 Jun 23; 30(25):2823–35. doi: [10.1038/onc.2011.10](https://doi.org/10.1038/onc.2011.10) PMID: [21317922](https://pubmed.ncbi.nlm.nih.gov/21317922/)
25. Stearns D, Chaudhry A, Abel TW, Burger PC, Dang CV, Eberhart CG. c-myc overexpression causes anaplasia in medulloblastoma. *Cancer Res*. 2006 Jan 15; 66(2):673–81. PMID: [16423996](https://pubmed.ncbi.nlm.nih.gov/16423996/)
26. Friedman HS, Burger PC, Bigner SH, Trojanowski JQ, Brodeur GM, He XM, et al. Phenotypic and genotypic analysis of a human medulloblastoma cell line and transplantable xenograft (D341 Med) demonstrating amplification of c-myc. *Am J Pathol*. 1988 Mar; 130(3):472–84. PMID: [3279793](https://pubmed.ncbi.nlm.nih.gov/3279793/)
27. Zhou L, Picard D, Ra YS, Li M, Northcott PA, Hu Y, et al. Silencing of thrombospondin-1 is critical for myc-induced metastatic phenotypes in medulloblastoma. *Cancer Res*. 2010 Oct 15; 70(20):8199–210. doi: [10.1158/0008-5472.CAN-09-4562](https://doi.org/10.1158/0008-5472.CAN-09-4562) PMID: [20876797](https://pubmed.ncbi.nlm.nih.gov/20876797/)
28. Khwaja A, Rodriguez-Viciano P, Wennstrom S, Warne PH, Downward J. Matrix adhesion and Ras transformation both activate a phosphoinositide 3-OH kinase and protein kinase B/Akt cellular survival pathway. *EMBO J*. 1997 May 15; 16(10):2783–93. PMID: [9184223](https://pubmed.ncbi.nlm.nih.gov/9184223/)

29. Irizarry RA, Bolstad BM, Collin F, Cope LM, Hobbs B, Speed TP. Summaries of Affymetrix GeneChip probe level data. *Nucleic Acids Res.* 2003 Feb 15; 31(4):e15. PMID: [12582260](#)
30. Eisen MB, Spellman PT, Brown PO, Botstein D. Cluster analysis and display of genome-wide expression patterns. *Proc Natl Acad Sci U S A.* 1998 Dec 8; 95(25):14863–8. PMID: [9843981](#)
31. Kool M, Koster J, Bunt J, Hasselt NE, Lakeman A, van Sluis P, et al. Integrated genomics identifies five medulloblastoma subtypes with distinct genetic profiles, pathway signatures and clinicopathological features. *PLoS One.* 2008; 3(8):e3088. doi: [10.1371/journal.pone.0003088](#) PMID: [18769486](#)
32. Northcott PA, Korshunov A, Witt H, Hielscher T, Eberhart CG, Mack S, et al. Medulloblastoma comprises four distinct molecular variants. *J Clin Oncol.* 2011 Apr 10; 29(11):1408–14. doi: [10.1200/JCO.2009.27.4324](#) PMID: [20823417](#)
33. Hagedorn M, Javerzat S, Gilges D, Meyre A, de Lafarge B, Eichmann A, et al. Accessing key steps of human tumor progression in vivo by using an avian embryo model. *Proc Natl Acad Sci U S A.* 2005 Feb 1; 102(5):1643–8. PMID: [15665100](#)
34. Ma L, Young J, Prabhala H, Pan E, Mestdagh P, Muth D, et al. miR-9, a MYC/MYCN-activated micro-RNA, regulates E-cadherin and cancer metastasis. *Nat Cell Biol.* 2010 Mar; 12(3):247–56. doi: [10.1038/ncb2024](#) PMID: [20173740](#)
35. Wu CH, Sahoo D, Arvanitis C, Bradon N, Dill DL, Felsher DW. Combined analysis of murine and human microarrays and ChIP analysis reveals genes associated with the ability of MYC to maintain tumorigenesis. *PLoS Genet.* 2008 Jun; 4(6):e1000090. doi: [10.1371/journal.pgen.1000090](#) PMID: [18535662](#)
36. Hart LS, Cunningham JT, Datta T, Dey S, Tameire F, Lehman SL, et al. ER stress-mediated autophagy promotes Myc-dependent transformation and tumor growth. *J Clin Invest.* 2012 Dec 3; 122(12):4621–34. doi: [10.1172/JCI62973](#) PMID: [23143306](#)
37. Roussel MF, Robinson GW. Role of MYC in Medulloblastoma. *Cold Spring Harb Perspect Med.* 2013 Nov; 3(11). doi: [10.1101/cshperspect.a015552](#) PMID: [24186492](#)
38. Chang TC, Zeitels LR, Hwang HW, Chivukula RR, Wentzel EA, Dews M, et al. Lin-28B transactivation is necessary for Myc-mediated let-7 repression and proliferation. *Proc Natl Acad Sci U S A.* 2009 Mar 3; 106(9):3384–9. doi: [10.1073/pnas.0808300106](#) PMID: [19211792](#)
39. Ball S, Li C, Li PK, Lin J. The small molecule, LLL12, inhibits STAT3 phosphorylation and induces apoptosis in medulloblastoma and glioblastoma cells. *PLoS One.* 2011; 6(4):e18820. doi: [10.1371/journal.pone.0018820](#) PMID: [21526200](#)
40. Hu Y, Liu CM, Qi L, He TZ, Shi-Guo L, Hao CJ, et al. Two common SNPs in pri-miR-125a alter the mature miRNA expression and associate with recurrent pregnancy loss in a Han-Chinese population. *RNA Biol.* 2011 Sep-Oct; 8(5):861–72. doi: [10.4161/rna.8.5.16034](#) PMID: [21788734](#)
41. Rhodes DR, Yu J, Shanker K, Deshpande N, Varambally R, Ghosh D, et al. ONCOMINE: a cancer microarray database and integrated data-mining platform. *Neoplasia.* 2004 Jan-Feb; 6(1):1–6. PMID: [15068665](#)
42. Pomeroy SL, Tamayo P, Gaasenbeek M, Sturla LM, Angelo M, McLaughlin ME, et al. Prediction of central nervous system embryonal tumour outcome based on gene expression. *Nature.* 2002 Jan 24; 415(6870):436–42. PMID: [11807556](#)
43. Wetmore C, Eberhart DE, Curran T. Loss of p53 but not ARF accelerates medulloblastoma in mice heterozygous for patched. *Cancer Res.* 2001 Jan 15; 61(2):513–6. PMID: [11212243](#)
44. Como D, Pala M, Cominelli M, Cipelletti B, Leto K, Croci L, et al. Gene signatures associated with mouse postnatal hindbrain neural stem cells and medulloblastoma cancer stem cells identify novel molecular mediators and predict human medulloblastoma molecular classification. *Cancer Discov.* 2012 Jun; 2(6):554–68. doi: [10.1158/2159-8290.CD-11-0199](#) PMID: [22628409](#)
45. Georger B, Kerr K, Tang CB, Fung KM, Powell B, Sutton LN, et al. Antitumor activity of the rapamycin analog CCI-779 in human primitive neuroectodermal tumor/medulloblastoma models as single agent and in combination chemotherapy. *Cancer Res.* 2001 Feb 15; 61(4):1527–32. PMID: [11245461](#)
46. Dudu V, Able RA Jr, Rotari V, Kong Q, Vazquez M. Role of Epidermal Growth Factor-Triggered PI3K/Akt Signaling in the Migration of Medulloblastoma-Derived Cells. *Cell Mol Bioeng.* 2012 Dec; 5(4):502–413. PMID: [24273611](#)
47. Liu J, Li JW, Gang Y, Guo L, Li H. Expression of leukemia-inhibitory factor as an autocrine growth factor in human medulloblastomas. *J Cancer Res Clin Oncol.* 1999 Aug-Sep; 125(8–9):475–80.
48. Trouillas M, Saucourt C, Guillotin B, Gauthereau X, Taupin JL, Moreau JF, et al. The LIF cytokine: towards adulthood. *Eur Cytokine Netw.* 2009 Jun; 20(2):51–62. doi: [10.1684/ecn.2009.0148](#) PMID: [19541590](#)

49. Dhingra K, Sahin A, Emami K, Hortobagyi GN, Estrov Z. Expression of leukemia inhibitory factor and its receptor in breast cancer: a potential autocrine and paracrine growth regulatory mechanism. *Breast Cancer Res Treat.* 1998 Mar; 48(2):165–74. PMID: [9596488](#)
50. Wysoczynski M, Miekus K, Jankowski K, Wanzeck J, Bertolone S, Janowska-Wieczorek A, et al. Leukemia inhibitory factor: a newly identified metastatic factor in rhabdomyosarcomas. *Cancer Res.* 2007 Mar 1; 67(5):2131–40. PMID: [17332343](#)
51. Baxter EW, Milner J. p53 Regulates LIF expression in human medulloblastoma cells. *J Neurooncol.* 2010 May; 97(3):373–82. doi: [10.1007/s11060-009-0043-x](#) PMID: [19907922](#)
52. David E, Tirode F, Baud'huin M, Guihard P, Laud K, Delattre O, et al. Oncostatin M is a growth factor for Ewing sarcoma. *Am J Pathol.* 2012 Nov; 181(5):1782–95. doi: [10.1016/j.ajpath.2012.07.023](#) PMID: [22982441](#)
53. Yu HG, Ai YW, Yu LL, Zhou XD, Liu J, Li JH, et al. Phosphoinositide 3-kinase/Akt pathway plays an important role in chemoresistance of gastric cancer cells against etoposide and doxorubicin induced cell death. *Int J Cancer.* 2008 Jan 15; 122(2):433–43. PMID: [17935137](#)
54. Ferretti E, De Smaele E, Po A, Di Marcotullio L, Tosi E, Espinola MS, et al. MicroRNA profiling in human medulloblastoma. *Int J Cancer.* 2009 Feb 1; 124(3):568–77. doi: [10.1002/ijc.23948](#) PMID: [18973228](#)
55. Ferretti E, De Smaele E, Miele E, Laneve P, Po A, Pelloni M, et al. Concerted microRNA control of Hedgehog signalling in cerebellar neuronal progenitor and tumour cells. *EMBO J.* 2008 Oct 8; 27(19):2616–27. doi: [10.1038/emboj.2008.172](#) PMID: [18756266](#)
56. Peng SC, Liao CT, Peng CH, Cheng AJ, Chen SJ, Huang CG, et al. MicroRNAs MiR-218, MiR-125b, and Let-7g Predict Prognosis in Patients with Oral Cavity Squamous Cell Carcinoma. *PLoS One.* 2014; 9(7):e102403. doi: [10.1371/journal.pone.0102403](#) PMID: [25050621](#)
57. Kotliarova S, Pastorino S, Kovell LC, Kotliarova Y, Song H, Zhang W, et al. Glycogen synthase kinase-3 inhibition induces glioma cell death through c-MYC, nuclear factor-kappaB, and glucose regulation. *Cancer Res.* 2008 Aug 15; 68(16):6643–51. doi: [10.1158/0008-5472.CAN-08-0850](#) PMID: [18701488](#)
58. Tan J, Li Z, Lee PL, Guan P, Aau MY, Lee ST, et al. PDK1 signaling toward PLK1-MYC activation confers oncogenic transformation, tumor-initiating cell activation, and resistance to mTOR-targeted therapy. *Cancer Discov.* 2013 Oct; 3(10):1156–71. doi: [10.1158/2159-8290.CD-12-0595](#) PMID: [23887393](#)
59. von Bueren AO, Shalaby T, Rajtarova J, Stearns D, Eberhart CG, Helson L, et al. Anti-proliferative activity of the quassinoid NBT-272 in childhood medulloblastoma cells. *BMC Cancer.* 2007; 7:19. PMID: [17254356](#)
60. Chesler L, Schlieve C, Goldenberg DD, Kenney A, Kim G, McMillan A, et al. Inhibition of phosphatidylinositol 3-kinase destabilizes Mycn protein and blocks malignant progression in neuroblastoma. *Cancer Res.* 2006 Aug 15; 66(16):8139–46. PMID: [16912192](#)
61. Kang S, Denley A, Vanhaesebroeck B, Vogt PK. Oncogenic transformation induced by the p110beta, -gamma, and -delta isoforms of class I phosphoinositide 3-kinase. *Proc Natl Acad Sci U S A.* 2006 Jan 31; 103(5):1289–94. PMID: [16432180](#)
62. Kang J, Rychahou PG, Ishola TA, Mourot JM, Evers BM, Chung DH. N-myc is a novel regulator of PI3K-mediated VEGF expression in neuroblastoma. *Oncogene.* 2008 Jun 26; 27(28):3999–4007. doi: [10.1038/onc.2008.15](#) PMID: [18278068](#)
63. Korshunov A, Remke M, Kool M, Hielscher T, Northcott PA, Williamson D, et al. Biological and clinical heterogeneity of MYCN-amplified medulloblastoma. *Acta Neuropathol.* 2012 Apr; 123(4):515–27. doi: [10.1007/s00401-011-0918-8](#) PMID: [22160402](#)
64. Ilic N, Utermark T, Widlund HR, Roberts TM. PI3K-targeted therapy can be evaded by gene amplification along the MYC-eukaryotic translation initiation factor 4E (eIF4E) axis. *Proc Natl Acad Sci U S A.* 2011 Sep 13; 108(37):E699–708. doi: [10.1073/pnas.1108237108](#) PMID: [21876152](#)